J. Hydrol. Hydromech., 64, 2016, 4, 316–328
DOI: 10.1515/johh-2016-0038

Experimental measurements for improved understanding and simulation of snowmelt events in the Western Tatra Mountains

Pavel Krajčí*, Michal Danko, Jozef Hlavčo, Zdeněk Kostka, Ladislav Holko

Institute of Hydrology, Slovak Academy of Sciences, Ondrašovská 17, Liptovský Mikuláš, Slovakia.
* Corresponding author. E-mail: krajci@uh.savba.sk

Abstract: Snow accumulation and melt are highly variable. Therefore, correct modeling of spatial variability of the snowmelt, timing and magnitude of catchment runoff still represents a challenge in mountain catchments for flood forecasting. The article presents the setup and results of detailed field measurements of snow related characteristics in a mountain microcatchment (area 59 000 m^2, mean altitude 1509 m a. s. l.) in the Western Tatra Mountains, Slovakia obtained in winter 2015. Snow water equivalent (SWE) measurements at 27 points documented a very large spatial variability through the entire winter. For instance, range of the SWE values exceeded 500 mm at the end of the accumulation period (March 2015). Simple snow lysimeters indicated that variability of snowmelt and discharge measured at the catchment outlet corresponded well with the rise of air temperature above 0°C. Temperature measurements at soil surface were used to identify the snow cover duration at particular points. Snow melt duration was related to spatial distribution of snow cover and spatial patterns of snow radiation. Obtained data together with standard climatic data (precipitation and air temperature) were used to calibrate and validate the spatially distributed hydrological model MIKE-SHE. The spatial redistribution of input precipitation seems to be important for modeling even on such a small scale. Acceptable simulation of snow water equivalents and snow duration does not guarantee correct simulation of peakflow at short-time (hourly) scale required for example in flood forecasting. Temporal variability of the stream discharge during the snowmelt period was simulated correctly, but the simulated discharge was overestimated.

Keywords: Snow accumulation and melt; Snowmelt rate; Snowmelt duration; Mountains; Snow lysimeter; MIKE-SHE.

INTRODUCTION

Snow accumulation and melt are highly variable in space and time (Pomeroy and Brun, 2001). Correct modeling of snowmelt spatial variability on catchment scale and catchment runoff still represent a challenge in mountainous river basins. Although floods caused solely by melting snow are not very frequent, rain on snow events are very often causes of large floods (Merz and Blöschl, 2003; Pekárová and Halmová, 2009). Improved knowledge on spatial variability of snow accumulation and melt transferred into better models may thus help with operational flood forecasting (Nester et al, 2012; Weingartner et al. 2003), reservoir management (Blöschl and Kirnbauer, 1991; DeWalle and Rango, 2008) or estimation of runoff changes in mountain areas caused by climate change impacts (Hlavčová et al., 2015; Kotríková et al., 2014; Zhang et al, 2015).

A lot of research on spatial variability of snow accumulation and snowmelt was conducted in the last decades. Numerous works were focused on the role of wind in snow accumulation in mountain environment above the treeline (Danko et al., 2014; Gray, 1979; Kuusisto, 1984; Lehning et al., 2008; Mott et al., 2010; Winstral et al., 2002, 2013). Balk and Elder (2000) used manual measurements and binary decision trees and geostatistical methods for estimation of snow cover distribution in non-forested area. Terrestrial laser scanning (TLS), airborne laser scanning or unmanned aerial systems (UAS) are newer approaches to measure spatial distribution of the snowpack. TLS and airborne LIDAR were tested by Prokop (2008) or Grünewald et al. (2010), respectively. Most of these methods are expensive and their deployment is time demanding. UAS was tested by De Michele et al. (2016). They concluded that UAS provides data with very high accuracy. However, the deployment is limited by meteorological conditions.

Other authors focused on modeling of snow redistribution affected by the wind, e. g. Winstral et al. (2002), Liston and Sturm (1998) or Vionnet (2012). Lehning et al. (2006) used the Alpine3D model to simulate snowpack processes and simulate runoff. The model provided very good runoff simulation, but it is very demanding from the point of view of the input data. Warscher (2013) used deterministic, spatially distributed hydrological model WaSiM-ETH for simulation of the discharge from snowmelt. Wind-driven snow distribution and energy balance scheme were integrated in the model. Energy balance with accounting for gravitational and wind-driven lateral snow redistribution led to the best accuracy.

Most of the above models were calibrated against snow water equivalent and runoff. However, model performance is rarely evaluated also by comparison with snowmelt outflow directly measured by snow lysimeters. Indeed, meltwater follows multiple flow paths downward through the snow and laterally into streams and rivers (Sturm, 2015) which reflect the small scale variability in solar radiation, sublimation, wind, as well as slope, aspect, exposure and the state and solid structure of the snowpack. Research connected with these devices has a long history. Construction of snow lysimeters is different, but the main idea is to provide measured data on melted water from a known area. It was used for example by Haupt (1969), Herrmann (1978), Greenan and Anderson (1984), Kattelmann (1984), Kuusisto (1984), Martinec (1987), Kirnbauer and Blöschl (1990), Tekeli et al. (2003), Holko et al. (2013), Elder et al. (2014). They were used not only for point measurements of meltwater outflow, but also for sampling of isotopic or chemical composition of snowmelt. Their application could gain a renewed interest in connection with the new remote sensing products. For example, the Sentinel observations of the European Space Agency provide the information about the snow wetness at 10–20 m resolution and the mapping algorithm needs to be tuned and validated.

The main objective of this work was to better understand the spatial and temporal patterns of snowmelt runoff generation in alpine (mountain) regions and test the network of measurements, we designed in a mountain microcatchment. Intensive field measurements included some snow-related data which are not routinely measured. Analysis of field data was complemented by spatially distributed hydrological modeling to check how precise can be a model which does not include snow transport and uses a relatively simple approach to calculate the snowmelt in simulation of spatial variability of the snow water equivalent and catchment runoff.

MATERIAL AND METHODS

Study area

Study area is located in the Western Tatra Mountains, northern Slovakia (Fig. 1). The microcatchment is the headwater area of the Sokolný creek. Its area is 0.059 km^2. The altitude ranges between 1450 m a. s. l. and 1560 m a. s. l. The bedrock is formed mainly by limestone and dolomite. Most of the catchment is covered by grass and low vegetation, young spruce forest occurs in its eastern part. Mean annual precipitation is about 1500 mm, mean air temperature is 3°C.

The study area is a subcatchment of the Jalovecký creek catchment which has measured data on snow depths and water equivalents since 1987 (Holko and Kostka, 2008). The data have been used in a number of studies devoted to various aspects of snow hydrology (Holko et al., 2011) including climate change and vegetation impacts (Holko et al., 2009b; Kostka and Holko, 2000), modelling (Holko et al., 2003, 2009a), remote sensing (Parajka et al., 2012; Krajčí et al., 2014) and isotopic studies (Holko et al., 2013; Penna et al., 2014).

Methods

The methodology combines snow-related data from field measurements in the catchment, climatic data measured near the catchment and modeling of catchment hydrological cycle by a spatially distributed rainfall-runoff model.

Field measurements

Snow water equivalent (SWE) and snow depth (SD) were measured in winter 2015 at 27 sites by the snow stakes (Figs. 1 and 2). Thirteen sites were located inside the catchment. Average distance between stakes was approximately 50 m. Fourteen sites were located outside the catchment, along its northwestern border. They were placed mainly on the ridge and the windward side considering the main direction of the winds in the area. SWE and SD were measured near each snow stake by the snow tube at least twice a month between January and April 2015.

Three snow lysimeters were installed in the catchment before the beginning of the snow season to provide data on snowmelt and its timing (Fig. 1). A simple construction designed to collect snowmelt water for our previous isotopic studies (Holko et al., 2013) was used (Fig. 2). The lysimeter consisted of a metallic pan with area 2068 cm^2 which collected snowmelt water and drained it into the tipping bucket gauge installed below it. The gauge was placed in a ground pit and covered with a polystyrene board to avoid water inflow from the snow covering the gauge. The gauge registered time of each tip. The pan was fixed to the ground by the nails inserted around it. Snow lysimeter measurements were validated by comparing total amount of melted water recorded by the lysimeter with the maximum snow water equivalent at a site.

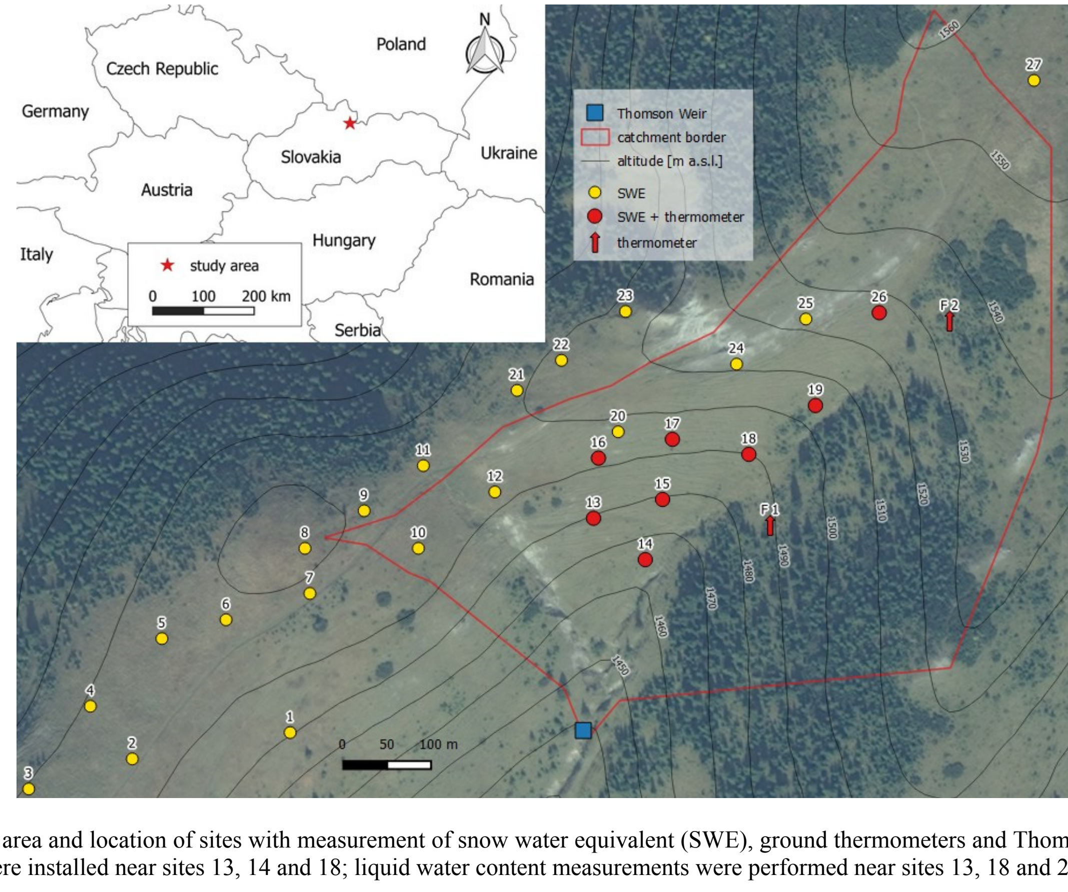

Fig. 1. Study area and location of sites with measurement of snow water equivalent (SWE), ground thermometers and Thomson weir; snow lysimeters were installed near sites 13, 14 and 18; liquid water content measurements were performed near sites 13, 18 and 26.

Fig. 2. Small snow lysimeter and snow stake. (length and width of the pan are 44, 47 cm respectively).

Liquid water content and snow density were measured in three snow pits by the Toikka Snow Fork device (Sihvola and Tiuri, 1986) at sites 13, 18 and 26 (Fig. 1). Expected accuracy of the device is ±0.5 vol.% (Sihvola and Tiuri, 1986). Five measurements during the winter were carried out at site 26 where the snow lasted longest. The width of the snow pits was about 80 cm. Liquid water content and snow density was measured every 10 cm from the soil surface up to the snow surface. Three measurements were carried out at each depth (on the left, in the middle and on the right side of the pit's wall) to account for the variability. Average value of these three measurements was then calculated for each depth.

Ten ground thermometers (EMS Minikin) were installed near the snow stakes on the soil surface to provide information on presence or absence of the snow cover (Fig. 1). Temperature was measured with an hourly time step. Static temperature close to 0°C (no rapid diurnal changes) indicated presence of the snow cover, i.e. the thermometer was buried under the snow. When the temperature rose above the freezing point or started to mimic the course of the air temperature, we concluded that the snow cover at the site completely melted. Data from thermometers were used to determine the duration of snow cover at a site.

Catchment runoff was measured by a V-notch weir (Fig.1). Water levels were measured hourly by pressure transducer. Correction of measured water levels for atmospheric pressure variability was based on data from a barometer placed near the weir. Streamflow at the weir is generated by the microcatchment alone and does not include contributions from outside of the catchment.

Automatic weather station located 500 meters from the microcatchment provided 10 min. data on precipitation, air temperature and solar radiation for the modeling. Long data series of snow water equivalent measurements on the site were used to characterize snow conditions of the studied winter.

The catchment was photographed during the snowmelt period, i.e. in second half of April, to obtain spatial patterns of patchy snow cover. Manual photographs were taken by the digital camera (Canon EOS 5D Mark II, lens with fixed focal length 50 mm). The photographs were compared with snow cover patterns simulated by the hydrological model.

Modeling

Spatially distributed rainfall-runoff model MIKE SHE coupled with the hydraulic river model MIKE 11 simulated hydrological cycle in the catchment. The model was run in an hourly time step from 1 November 2014 until 21 July 2015.

Model inputs included precipitation, air temperature, solar radiation measured at the weather station near the catchment. Topography was incorporated by the digital elevation model with resolution 5 meters. Potential evapotranspiration was calculated in the daily step by the Blaney-Criddle method (Schrödter, 1985).

Snow accumulation was simulated by a common approach using the threshold air temperature. All precipitation, that fell when the air temperature was below the threshold was supposed to be solid. This model parameter was calibrated. The same threshold temperature was used to initiate the beginning of the snowmelt if the measured air temperature was above the threshold. Snowmelt simulation was based on the degree-day approach, but the energy of incoming liquid precipitation and radiation melt were considered as well. Partial snow coverage of the grid cells was not considered in the simulation. Variable degree-day factors given in Table 1 were used. These values were calculated according to the long term observations in the Jalovecký creek catchment analyzed in Holko et al. (2012). Eighteen model parameters were calibrated (e.g. snow melt, hydraulic conductivity, etc.). Parameter characterizing maximum wet snow fraction was set to 8.76% according to Snow Fork measurements of liquid water content. The model did not account for snow redistribution by the wind.

Table 1. Variable degree day factors used in the modeling.

Date (from)	Degree-day factor [mm.°C^{-1}.day^{-1}]
1 November	1
31December	0.55
30 January	1.85
28 February	4.12
15 March	7

Snow melting and freezing

Snow melts in response to several characteristics, including air temperature, solar radiation, the heat content of rain, and the heat transfer from condensing moisture in the air.

Snow moisture content

It is well known that melting snow does not immediately generate runoff. Rather, the snow gradually becomes wetter, until liquid water starts to drain out of the snow pack (MIKE-SHE, 2011). If the temperature drops below freezing again, the liquid water will re-freeze. In MIKE SHE, this is conceptualized as two separate snow storages - dry (or frozen) snow storage and wet (or liquid) snow storage (MIKE-SHE, 2011). Snow melt occurs by converting dry snow to wet snow. Surface runoff occurs when the ratio of dry to wet snow storage reaches a user specified maximum - the maximum wet snow storage fraction, where the wet snow storage fraction, W_{frac}, is calculated by

$$W_{frac} = \frac{S_{wet}}{S_{wet} + S_{dry}}$$

where S_{wet} and S_{dry} are the wet and dry snow storages respectively.

Air temperature melting

If the air temperature is above the threshold melting temperature, then the snow will begin to melt and the snow storage will be reduced by

$$M_T = C_T\left(T_{air} - T_0\right)$$

where M_T is the rate of melting due to the air temperature, C_T is the degree-day factor for snow melting (e.g. in units of mm/day/C degree), T_{air} is the air temperature of the cell, and T_0 is the threshold melting temperature. The air temperature melting will be positive if the air temperature is above the threshold temperature and negative if it is below. Thus, if the air temperature falls below the threshold melting temperature, then wet snow will be reconverted back to dry snow. In MIKE SHE, the degree-day factor is a time varying, spatially distributed value.

Radiation melting

Solar radiation will cause the snow to melt at a rate proportional to the amount of incoming radiation. On cloudy days, the radiation intensity will be less, but still non-zero. Thus,

$$M_R = -C_{rad}\, R_{sw}$$

where M_R is the rate of melting due to incoming short wave radiation, C_{rad} is the radiation melting factor for snow melting (e.g in units of mm/kJ/m^2), R_{sw} is the amount of incoming solar radiation (e.g. in units of kJ/m^2/hour).

Energy melting

The condensation of moist air on snow and the heat released from liquid rain as it cools are important contributors to snow melt. Even though these energy sources are not physically simulated, the following linear relationship allows these processes to be included.

$$M_E = C_E\ P\left(T_{air} - T_0\right)$$

where M_E is the rate of melting due to the energy in liquid rain, C_E is the energy melting coefficient for the energy in liquid rain (e.g. in units of mm/mm rain/C degree), T_{air} is the air temperature of the cell, and T_0 is the threshold melting temperature. Energy melting only occurs if the air temperature is above the threshold melting temperature. The temperature of the rain is assumed to be the same as the air temperature. The energy melting coefficient is a constant value for the entire model.

Snow balance

If the air temperature is above the threshold melting temperature, then dry snow storage will be reduced (converted to wet snow) by combining the three melting rates.

$$M_{total} = M_T + M_R + M_E$$

If, on the other hand, the air temperature is below the threshold melting temperature, then the dry snow storage will be increased (wet snow converted to dry snow) by combining the freezing rate and the radiation melting rate, until the wet snow storage goes to zero

$$T_{total} = M_T + M_R$$

In this case, the temperature melting will be positive and radiation melting will be negative (MIKE SHE, 2011).

Precipitation and air temperature are the key input data determining simulation of snow accumulation, timing and rate of snowmelt and also simulated catchment runoff. We assumed that spatially uniform precipitation and air temperature measured by the nearby weather station can be used as input data due to small catchment area. However, preliminary work with the model showed that precipitation would have to be distributed to obtain reasonable simulation of snow water equivalent. Thiessen polygons constructed around the 13 snow stakes located in the catchment were used to redistribute precipitation amounts measured at the weather station. The weights attributed to the polygons were calculated from the snow distribution measured at the time of maximum SWE on 5th March 2015. Spatial distribution of air temperature was based on the altitude gradient whereby the lapse rate 0.649°C per 100 m of altitude was used. Our unpublished long term data from the Jalovecká creek catchment indicate that this value approximately represents maximum seasonal value which is on average observed in spring and early summer.

Snow water equivalents measured at the snow stakes located inside the catchment and catchment runoff were used in model calibration. Except visual check of plausibility, the Nash-Sutcliffe coefficient (Nash and Sutcliffe, 1970) and the root mean square error were used to optimize the simulations. Multiobjective calibration was performed, three objectives were considered (discharge, snow melt and SWE). Calibration strategy was focused on the best possible simulation of SWE maximum and snowmelt duration (time of snow disappearance) using the trial and error approach and visual evaluation of the results. Accurate simulation of catchment peakflows had smaller priority, but we strived to reproduce runoff variability as good as possible. Comparison of simulated snow cover duration with that derived from ground thermometers was used in the assessment of model performance. We also qualitatively compared snow patterns simulated by the model and given by ground photographs and measured and simulated outflow from the snow cover.

RESULTS

Snow conditions in winter 2015

Long term measurements of SWE and SD at the weather station showed that snow conditions during winter 2015 were approximately average. Maximum snow water equivalent at the weather station was measured on 10th April 2015 and reached 404 mm. This value is identical with the long-term mean of SWE maxima for winters 1996–2015. The first snowfall occurred at the beginning of December 2014, but the snow cover quickly melted. Snow accumulation period started in the middle of December 2014. The first pronounced snowmelt in the study area started on 17th March 2015 when the air temperature rose above 5°C (Fig. 3). Significant snowmelt occurred after 25th March when the air temperature exceeded 10°C. Air temperature decreased at the beginning of April and new snow cover accumulated with maximum on 10th April. Gradual snowmelt continued after that and the snow cover almost completely melted in the catchment approximately until the end of April.

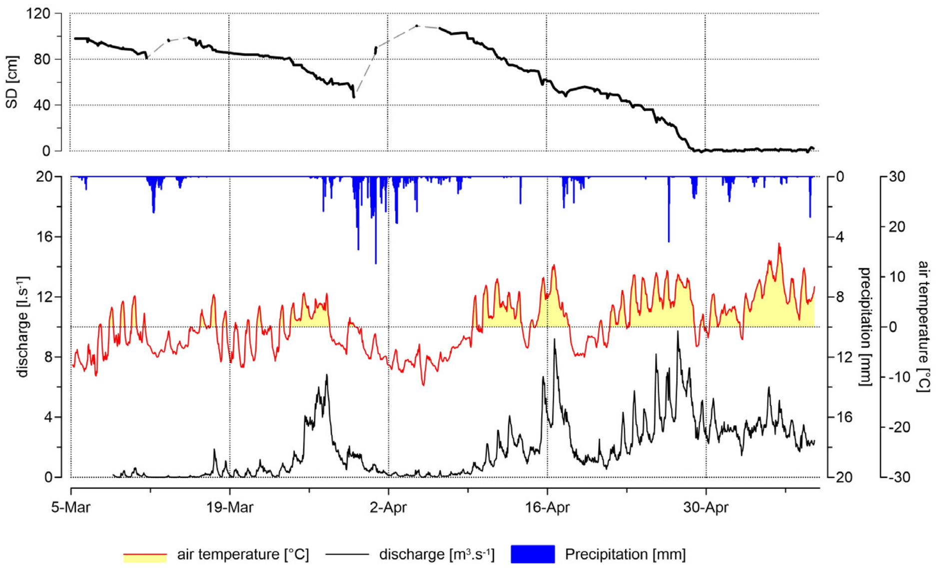

Fig. 3. Meteorological and hydrological situation during the snowmelt period 2015; top panel – temporal variability of SD measured by the ultrasonic sensor at weather station; bottom panel - precipitation and air temperature at the weather station and catchment discharge.

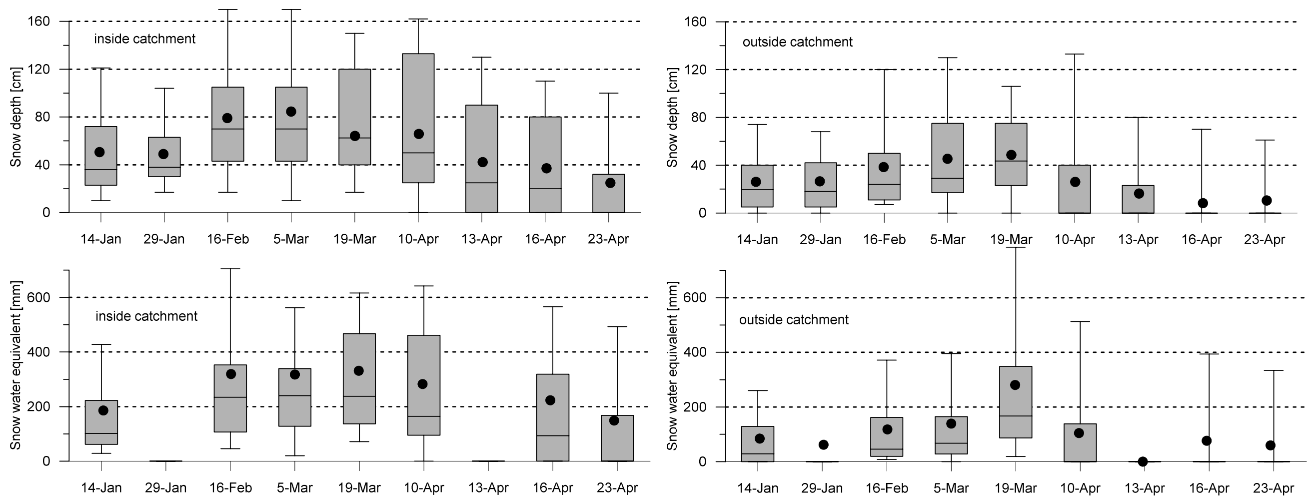

Fig. 4. Variability of spatial distribution of SD and SWE; the whiskers show minimum and maximum on particular day, the boxes represent the first and third quartiles; median is indicated by the line inside the boxes; the black circle represents arithmetic means based on 13 measurements inside the catchment and 14 measurements outside it.

Table 2. Snow water equivalents [mm] at snow stakes located inside the catchment during the maximum accumulation.

No.	10	12	13	14	15	16	17	18	19	20	24	25	26
5.3.2015	90	330	240	128	339	562	91	209	290	149	20	545	543
19.3.2015	72	273	203	163	378	530	94	137	359	116	0	467	616

Table 3. Snow water equivalents [mm] at snow stakes located outside the catchment during the maximum accumulation.

No.	1	2	3	4	5	6	7	8	9	11	21	22	23	27
5.3.2015	396	19	85	29	26	99	256	28	159	321	38	50	0	165
19.3.2015	398	<10	87	69	<10	<10	282	<10	177	349	19	<10	<10	157

Variability of snow accumulation and melt based on measured data

Variability of SD and SWE inside the catchment and along its border (outside the catchment) is shown in Fig. 4. All values measured during time of maximum SWE are given in Tables 2 and 3. The ranges of values in the catchment are high through the entire season. They are smaller for sites located outside catchment. These sites have much less snow due to wind erosion and blowing snow. However there are sites with little snow also in the catchment (Table 2). Big differences between the arithmetic mean and median were found for most days with measurements (Fig. 4).

Different sites reached the maximum SWE on different days. For example, maximum was measured at sites 25 and 26 in the beginning of April while at site 15 it was measured already in the beginning of March. Sites located on the ridge, e.g. 5 or 24, did not have one clear maximum. SWE at these sites never exceeded 100 mm. The highest differences within the catchment occurred on 5th March 2015 when the SWE ranged between 20–562 mm (Table 2). The highest values were measured at sites 16, 25 and 26. SWE higher than 300 mm was measured at these sites even on 23rd April 2015, when most of the catchment was already without snow. These sites are located on leeward southeast side of the ridge. The snow drift which regularly forms in that part of the catchment indicates lower wind speeds.

Measurements of SD and SWE can be used in assessment of differences in spatial variability of snowmelt as well. An indirect assessment based on ground temperature can be useful. Ten thermometers installed on the ground surface allowed a rather accurate estimate of whether the particular site was snow covered or snow free. Most of the sites were continuously covered with snow from 17th December until second half of April (Fig. 5). Site 17 was an exception because the snow completely melted there also on 26th of March when longer period of warmer temperatures occurred. Later in April when another warm period appeared, it was the first site which became snowless (on 13th April). This was also confirmed by a photograph taken on 14th April (Fig. 6). The longest snow duration was indicated by ground air temperature for site 26. Snow cover completely melted there just in the beginning of May. The above differences in snowmelt duration have two reasons. The first one is that site 17 is more exposed to solar radiation than site 26. The difference between the two sites in sum of the potential solar radiation for period 16th–25th March reached 10 000 Wh m^{-2} (Fig. 6 right). The second reason of the differences is related to smaller amount of snow accumulated at the site which is confirmed by comparison of sites 17 and 16. Site 16 was also exposed to high solar radiation (Fig. 6 left), but the amount of accumulated snow expressed by SWE was much higher there (Table 2).

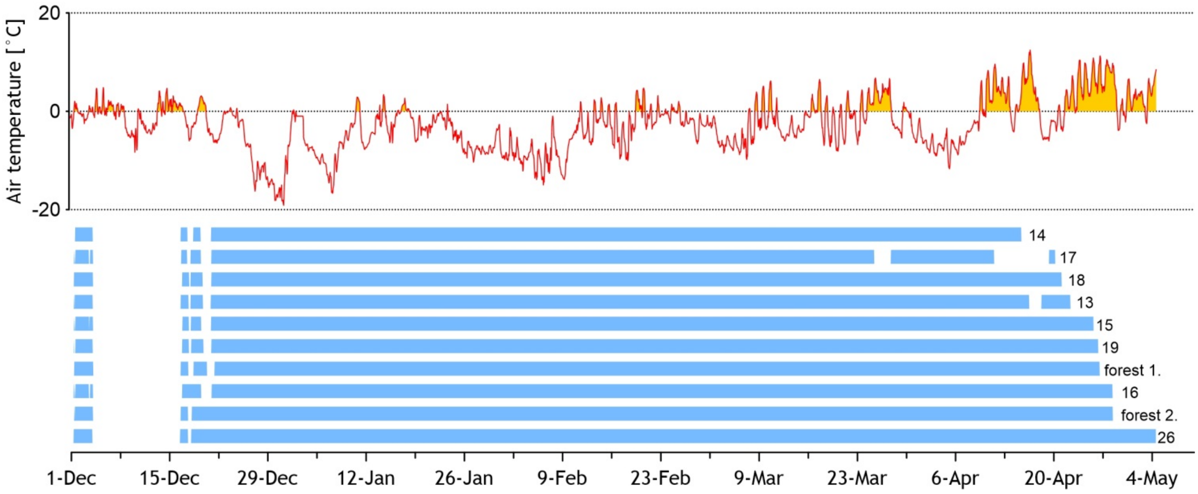

Fig. 5. Air temperature measured at weather station (the top panel) and snow cover duration given by ground thermometers at different sites (stripes in the bottom panel).

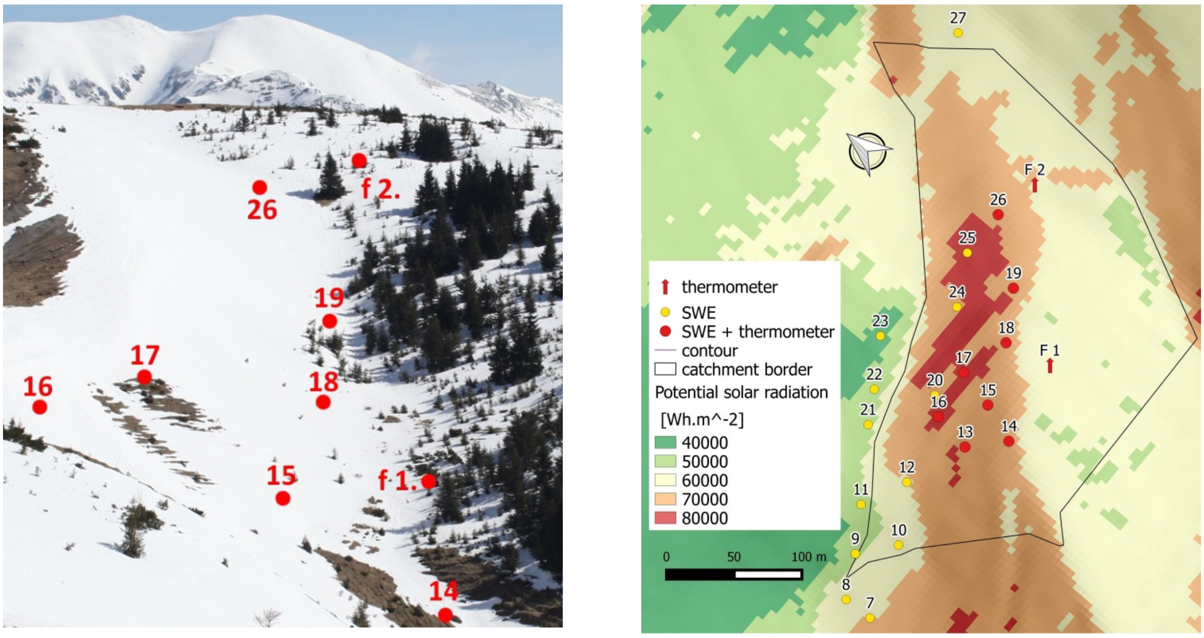

Fig. 6. Photo of the catchment on 14th April 2015 (left panel) and sum of potential solar radiation calculated for 16–25 March according to Mészároš and Miklánek (2006), i.e. period of significant snowmelt (right panel); the red dots in the right panel show sites with measurements of ground temperature.

Snow lysimeters were tested as another approach to estimate spatial and temporal variability of snowmelt.

Data from the third lysimeter located at site 14 are most realistic. The first melt was recorded on 8th March, when the air temperature significantly raised above 0°C. Snowmelt outflow was very small. More important melting began on 17th March (Fig. 7). Hourly maxima of snowmelt varied mostly between 1 and 3 millimeters, but an extraordinary melt of 5 mm per hour was recorded on 25th April. The degree-day factors at this site calculated for the days without precipitation varied between 2.6 and 9.8 mm °C day^{-1}; the mean was 6.0 mm °C day^{-1}.

Snowmelt occurrence measured by the lysimeter corresponded to changes of discharges measured at catchment outlet. Catchment runoff peaks occurred after the snowmelt outflow peaks measured by the snow lysimeter with the delay of about 2 hours. Daily amplitudes of catchment discharges were smaller than those of lysimeters. Catchment daily runoff during the snowmelt period varied between 0 and 9.2 mm. Daily minima occurred early in the morning (at 4–5 a.m.), maxima in the afternoon (at 2–4 p.m.). Diurnal variability of catchment runoff correlated well with that of the air temperature.

Spatial variability of snowmelt outflow could not have been evaluated because two of three installed lysimeters provided suspicious data, i.e. unrealistically high outflow or almost no response. We assume that the suspicious measurements had two reasons. The first one was related to the location. The lysimeter was located at a site where the slope of the terrain declined. As a result, larger volume of meltwater from the upslope area was drained to the lysimeter. The second reason of unrealistic data (no response) was caused by clogging of the measuring gauge with grass and other material.

Variability of snow accumulation and melt affects also the amount of liquid water present in the snow cover. Maximum amount of liquid water held by the snow is a parameter of the snowmelt models which is usually fixed. Our measurements show that snow contained very little water in February and in the beginning of March (Fig. 8). Increased wetness was measured on 10th April when the fresh snow on the surface was dry, but the snow cover below it contained around 4% of water. Only pit at site 26 provided data in the second half of April. Most of the snowpack contained approximately 4 to 6% of water, but the very top and bottom layers were much wetter (Fig. 8).

Modeling

Simulated snow water equivalents at eight of thirteen snow stakes (12 to 16, 18, 19 and 24) were quite similar to the measured ones (Fig.9). These sites are located in the lower part of the catchment and the model reasonably simulated also the time of complete snow disappearance (mean RMSE = 58 mm). SWE simulation was worse for sites with significant snow drift, e.g. 25 and 26. Simulated snow water equivalent during the accumulation period was underestimated there and the model simulated earlier disappearance of the snow cover at those sites. Simulated SWE was overestimated at sites 10 and 17.

Simulation of snow cover duration was good for most sites except sites 16 and 17 where the complete disappearance of snow was simulated 7 and 5 days earlier, respectively. Simulated spatial patterns of snow cover are compared with photographs in Fig. 10. Although the simulated patterns in the open area corresponded to the photographs rather well they were clearly affected by the method of precipitation redistribution (Thiessen polygons).

Simulated point snowmelt did not always correspond to snow lysimeter data (Fig. 11). While the snow lysimeter measured uninterrupted outflow from the snow cover for a period of several days, simulated snowmelt indicated several discrete snowmelt water inputs at the site. The difference in total simulated and measured snowmelt was 20%.

Although the SWE and snow cover duration at most sites were simulated relatively well, simulation of catchment runoff was not so successful (Fig. 11). Short-time runoff variability visible in hourly data was not reproduced. Timing and peak of the first larger snowmelt event was simulated very well, but the following events were overestimated although the timing of hydrograph components (rising and falling limps, peakflow) corresponded to measured data. Possible future model improvements are discussed in the following section.

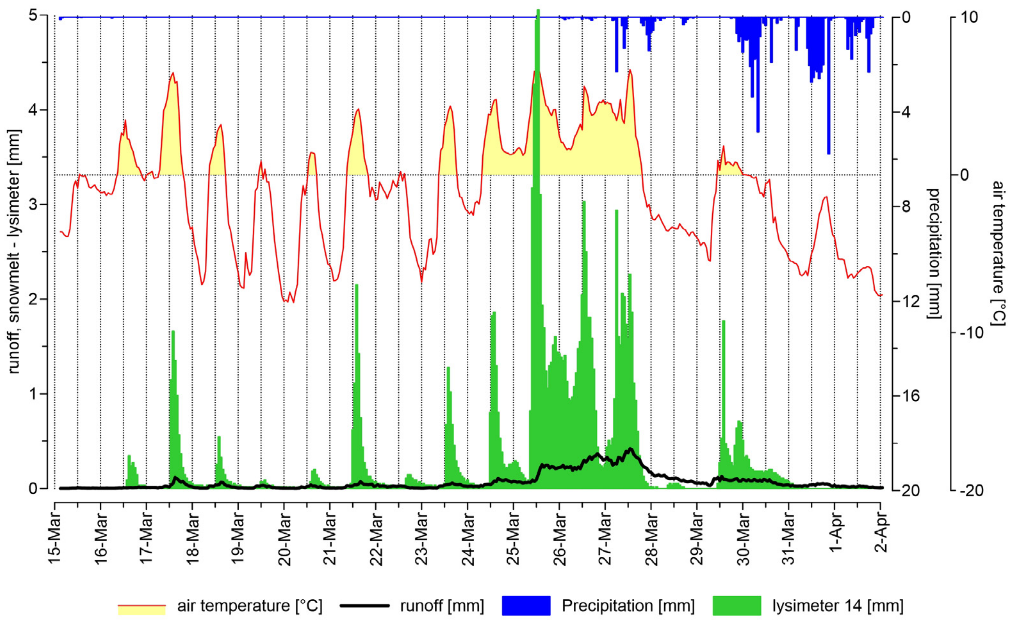

Fig. 7. Hourly precipitation, air temperature, snowmelt lysimeter outflow and catchment runoff in the second half of April 2015; the gridlines are drawn every 12 hours.

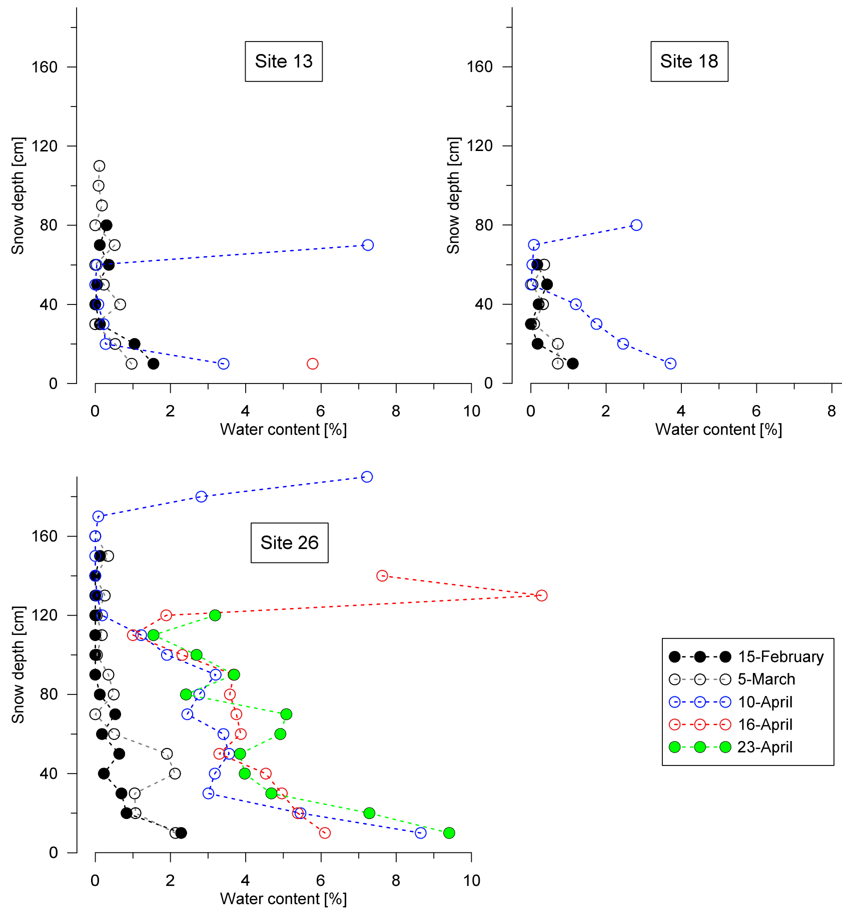

Fig. 8. Water content of snow during the season measured in three snow pits.

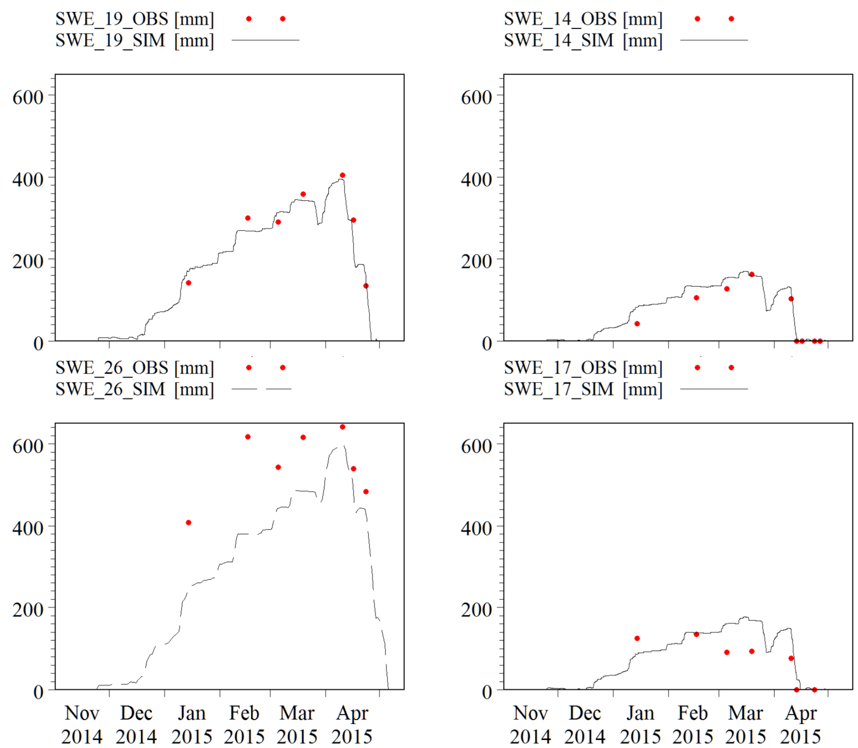

Fig. 9. Measured (OBS) and simulated (SIM) snow water equivalents at different sites; good simulation for sites 19 and 14, underestimated SWE for the snow drift affected site 26 and overestimated SWE at site 17 with little snow accumulation and high income of solar radiation.

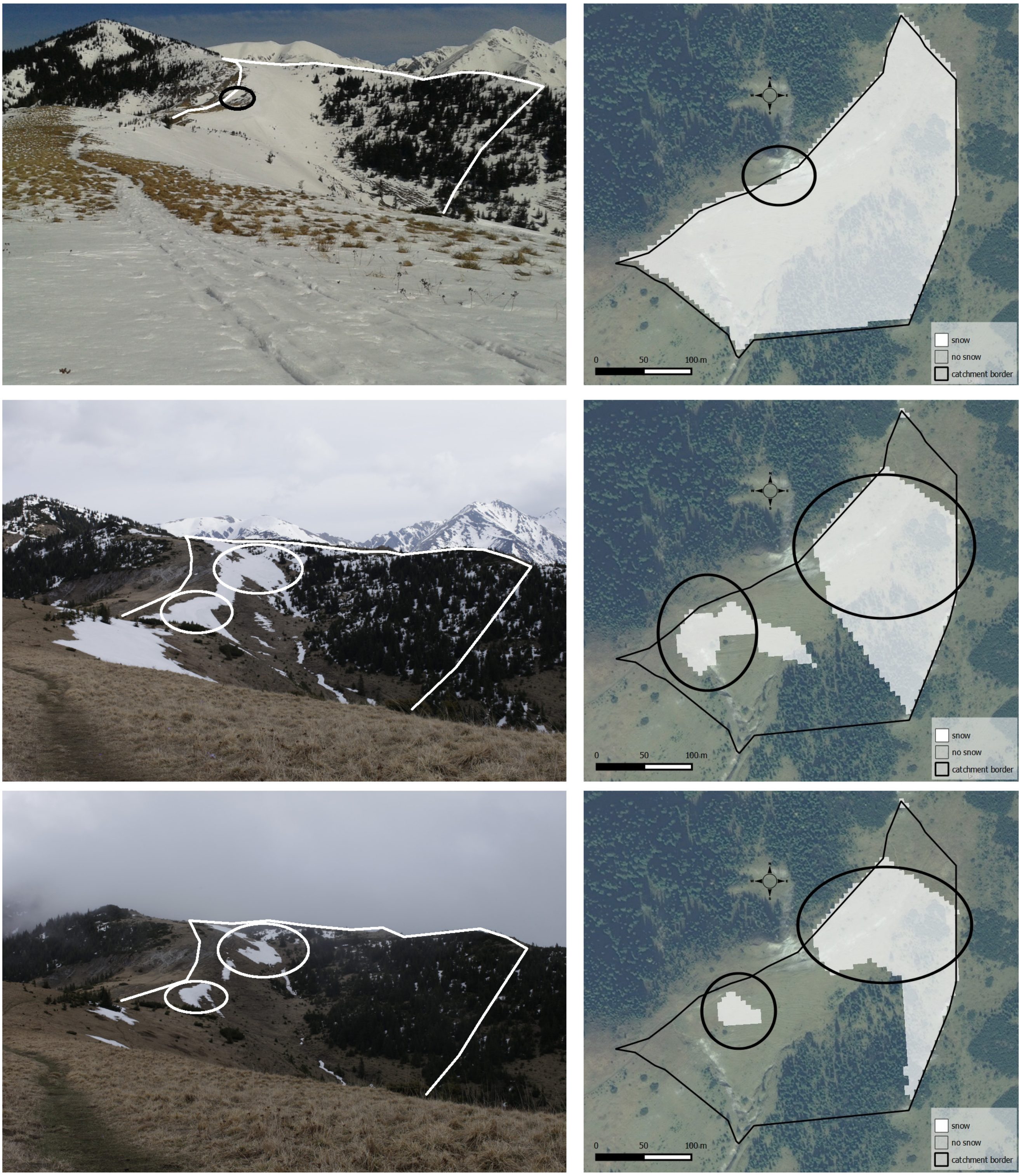

Fig. 10. Comparison of snow patterns from photographs (left) and model (right) on 10 April, 26 April and 2 May (from top to bottom).

DISCUSSION AND CONCLUSIONS

The study provided several data sets which are useful in description of spatial and temporal variability of snow accumulation and melt in a mountain catchment. Field (manual) measurements of snow depth and water equivalent provide the most accurate data, especially in mountains (e.g. Khan and Holko, 2009). Large spatial variability of snow characteristics found in our study area is in agreement with the results presented e.g. by López-Moreno et al. (2013). Significant difference between mean and median values indicates that mean values should be used with care for characterization of snow storage in catchments with complex topography. We used boxplots to characterize the variability. More detailed analysis of the links with terrain features or vegetation (e.g. Hríbik et al., 2012) needs to be done in future studies. Revuelto et al. (2014) concluded that topographic position index TPI helped explain variability of SD distribution. TPI at a 25 m searching distance was the best variable explaining snow depth distribution in their experimental catchment. Maximum upwind slope was also an important variable.

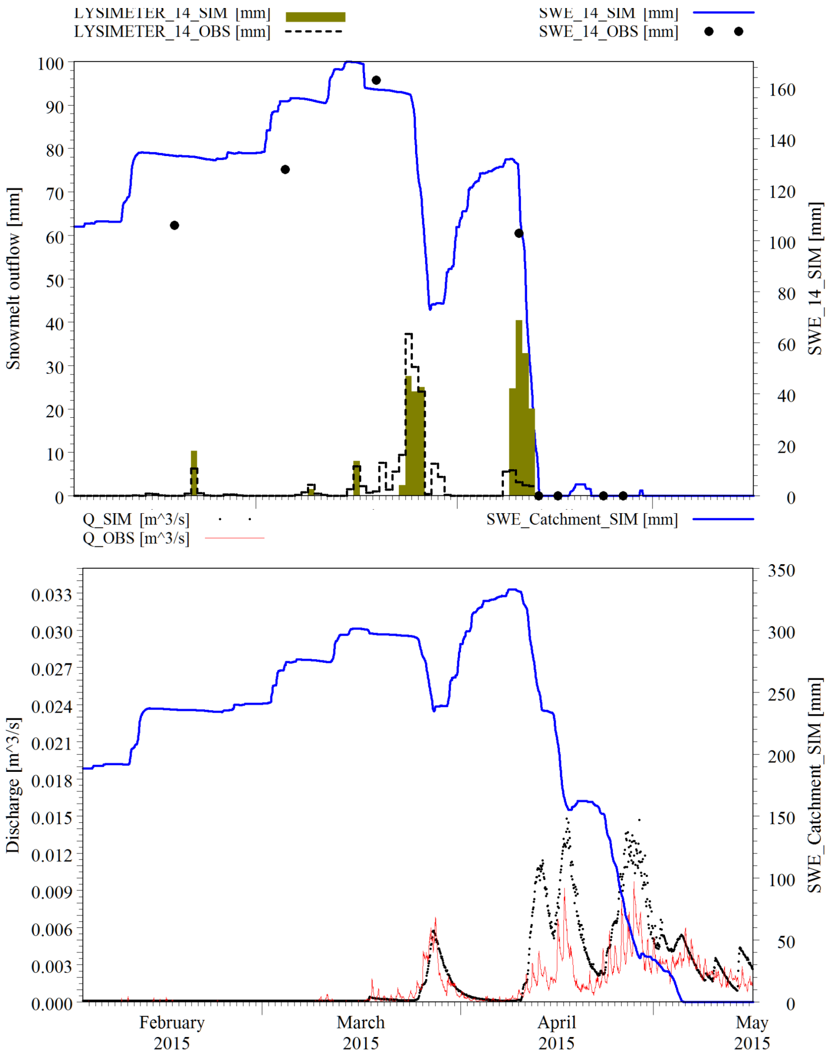

Fig. 11. Measured and simulated SWE at site 14 where the snow lysimeter was installed and comparison of measured and simulated outflow from melting snow (the top panel); simulated catchment mean SWE and comparison of measured and simulated catchment runoff (the bottom panel). Red line - Q observed. Dotted line - Q simulated.

Spatial density of measured points and frequency of field measurements of SD and SWE may not always be adequate to the purpose of a study. Information on snow duration obtained from ground thermometers can significantly improve the knowledge of spatial variability of snow disappearance at smaller scales. Ground thermometers are relatively cheap and can be easily employed in snow studies as shown by Lundquist and Lott (2008). Our experience confirms the usefulness of such data in process study as well as in modeling.

Snow lysimeters provide unique information about the process of snowmelt. The simple design used in our study proved to be useful and cheap. However, proper installation is important to avoid problems with unrealistic data. The rain gauges used in this study had very thin tubes connecting the funnel with the tipping bucket. As a result, one gauge was clogged with material brought by the snowmelt water and did not provide correct data.

The degree-day factor values between 2.6 and 9.8 mm °C day^{-1} measured by the snow lysimeter are mostly in agreement with the values proposed in Hock (2003) and Kuusisto (1980). Just the maximum value of 9.8 mm °C day^{-1} was slightly higher than the values provided in the above-mentioned articles. It can be caused by the exposition of the site and therefore high values of incoming solar radiation.

Snow wetness is not commonly measured in snow hydrology research although several recent papers presented the development of some new devices and modeling of liquid water content of snowpack (Avanzi et al., 2014, 2015). Examples of other new devices are Heilig et al. (2015), or Kinar and Pomeroy (2015), while Hirashima et al. (2014) or Wever et al. (2014) discuss the new modeling methods. In this study we have used the Snow Fork in snow pits. Such an approach does not identify only the extremely wet layers (snow surface and soil-snow boundary in our study area where the soils rarely freeze). It also allows determination of prevailing water content of the bulk of snowpack which was smaller than the extreme values. However, the snow pit approach is time demanding and therefore cannot provide spatially distributed data with higher temporal frequency of measurements. Furthermore, it is invasive which may be of importance at small scales and during time of intensive snowmelt. Toikka (2013) reported that values exceeding 10% might be inaccurate. Our measurements indicated just one such value measured at the end of the snowmelt season. Other values were in the range when the equipment should work reliably.

Main focus of our study were manual, snow-related measurements and their analysis, but we also wanted to test the possibilities of assimilation of the measured data in hydrological model with simulation step relevant to flood forecasting applications, i.e. the hourly time step. It is obvious that confirmation of model usability would need longer data series and more focus on validation. The model used in the study could reasonably reproduce measured snow water equivalents at most sites. Larger differences were encountered at places with significant snow drift and sites with little snow exposed to high solar radiation. Simulated snow cover patterns resembled to those obtained from the photographs. Point snowmelt did not always correspond to measurements of snow lysimeter. Temporal variability of catchment runoff was simulated correctly for the first bigger snowmelt event although the short-time runoff changes were not reproduced. However, runoff amount was often overestimated. The overestimation may be connected with deep water percolation affected by geology (limestone and dolomite) or by incorrect precipitation data which was measured outside the catchment (although the weather station was very close to the catchment). In fact, spatial redistribution of precipitation seems to be very important even at this small scale (59 000 m^2). Our further work will therefore focus on improved redistribution of precipitation. For example, Kormos et al. (2014) used wind corrected precipitation using method introduced in Winstral et al. (2013). The method is based on measurements of maximum upwind slopes and upwind breaks inslope in direction of most prevailing wind direction. Improved precipitation pattern should also improve spatial patterns of snow cover simulated by the model. More attention should also be paid to objective functions optimizing SWE modeling at all snow stakes. Improvement of simulated runoff can be achieved not only by the improvement of the spatial distribution of precipitation but also by a better parametrization of other processes of runoff formation. Our modeling results show that acceptable simulation of SWE does not guarantee correct modeling of catchment runoff at time scales needed in flood forecasting.

Presented experimental network provided various data sets related to spatial variability of snow accumulation and melt. Field measurements allow improved validation of hydrological models and point at uncertainties which should be addressed in model development. Additional effort needs to be devoted to preparation of spatially distributed input precipitation for the model. Analysis of the obtained data was used in an extended design of field measurements for another winter season.

Acknowledgements. This work was supported by grant VEGA 2/0055/15.

REFERENCES

Avanzi, F., Caruso, M., Jommi, C., De Michele, C., Ghezzi, A., 2014. Continuous-time monitoring of liquid water content in snowpacks using capacitance probes: A preliminary feasibility study. Advances in Water Resources, 68, 32–41.

Avanzi, F., Yamaguchi, S., Hirashima, H., De Michele, C., 2015. Bulk volumetric liquid water content in a seasonal snowpack: modeling its dynamics in different climatic conditions. Advances in Water Resources, 86, 1–13.

Balk, B., Elder, K., 2000. Combining binary decision and geostatistical methods to estimate snow distribution in a mountain watershed. Water Resources Research, 36, 1, 13–26.

Blöschl, G., Kirnbauer, R., 1991. Point snowmelt models with different degrees of complexity - internal processes. Journal of Hydrology, 129, 127–147.

Danko, M., Krajčí, P., Hlavčo, J., 2014. Vzťah výšky snehovej pokrývky a vodnej hodnoty snehu v lese a na voľnej ploche v povodí Jaloveckého potoka. [The relationship between snow depth and snow water equivalent in the forest and in the open area in the Jalovecký creek catchment]. Acta Hydrologica Slovaca, 15, 1, 116–128. (In Slovak.)

De Michele, C., Avanzi, F., Passoni, D., Barzaghi, R., Pinto, L., Dosso, P., Ghezzi, A., Gianatti, R., Della Vedova, G., 2016. Using a fixed-wing UAS to map snow depth distribution: an evaluation at peak accumulation. The Cryosphere, 10, 511–522. doi:10.5194/tc-10-511-2016.

DeWalle, D.R., Rango, A., 2008. Principles of Snow Hydrology. Cambridge University Press, Cambridge.

Elder, K., Marshall, H. P., Elder, L., Starr, B., Karlson, A., Robertson, J., 2014. Design and installation of a tipping bucket snow lysimeter. In: Proc. Int. Snow Science Workshop, ISSW steering committee, Banff, pp. 817–824.

Gray, D.M., 1979. Snow accumulation and distribution. In: Colbeck, S.C., Ray, M. (Eds.): Proc. Modeling of snow cover runoff, J. S. Army Cold Regions Research and Engineering Laboratory, Hanover, N.H., pp. 3–33.

Greenan, H.J., Anderson, E.A., 1984. A snowmelt lysimeter for research applications. In: Elhadi, N.D., Frechette, M.A. (Eds.): Proc. 41 Annual Eastern Snow Conference, Eastern Snow Conference, Washington, D.C., pp. 212–216.

Grünewald, T., Schirmer, M., Mott, R., Lehning, M., 2010. Spatial and temporal variability of snow depth and SWE in a small mountain catchment. Cryosphere, 4, 1–11.

Haupt, H.F., 1969. A simple snowmelt lysimeter. Water Resources Research, 5, 3, 714–718.

Heilig, A., Mitterer, C., Schmid, L., Wever, N., Schweizer, J., Marshall, H.P., Eisen, O., 2015. Seasonal and diurnal cycles of liquid water in snow – Measurements and modeling. J. Geophysical Research Earth Surface, http://dx.doi.org/10.1002/2015JF003593

Herrmann, A., 1978. A recording snow lysimeter. Journal of Glaciology, 20, 82, 209–213.

Hirashima, H., Yamaguchi, S., Katsushima, T., 2014. A multidimensional water transport model to reproduce preferential flow in the snowpack. Cold Regions Sci. Technol., 108, 80–90. http://dx.doi.org/10.1016/j.coldregions.2014.09.004

Hlavčová, K., Kotríková, K., Kohnová, S., Valent, P., 2015. Changes in the snow water equivalent in mountainous basins in slovakia over recent decades. IAHS Publ. No. 370, IAHS Press, Wallingford, pp. 109–116.

Hock, R., 2003. Temperature index melt modelling in mountain areas. J. Hydrol., 282, 104–115. doi: 10.1016/S0022-1694(03)00257-9.

Holko, L., Kostka, Z., 2008. Hydrological characteristics of snow cover in the Western Tatra Mountains in winters 1987–2008. Folia Geographica, Series Geographica-Physica, vol. XXXIX, 63–77.

Holko, L., Kostka, Z., Parajka, J., 2003. Distributed snow water equivalent modeling in a mountain catchment. Journal of Hydrology and Hydromechanics, 51, 1, 39–51.

Holko, L., Sokratov, S.A., Shmakin, A.B., Kostka, Z., 2009a. Simulation of snow water equivalent by mathematical models of different complexity. Materialy Glyatsiologicheskikh Issledovanii, no. 107, 72–80. ISSN 0145 8752.

Holko, L., Škvarenina, J., Kostka, Z., Frič, M., Staroň, J., 2009b. Impact of spruce forest on rainfall interception and seasonal snow cover evolution in the Western Tatra Mountains, Slovakia. Biologia 64, 3, 594–599. doi: 10.2478/s11756-009-0087-6.

Holko, L., Gorbachova, L., Kostka, Z., 2011. Snow Hydrology in Central Europe. Geography Compass, 5, 4, 200–218. doi: 10.1111/j.1749-8198.2011.00412.x.

Holko, L., Danko, M., Kostka, Z., 2012. Klasifikácia zím, hustota nového snehu a teplotný faktor topenia snehovej pokrývky v povodí Jaloveckého potoka. [Classification of winters, density of new snow and the degree-day factor in the Jalovecký creek catchment]. Acta Hydrologica Slovaca, 13, 2, 342–349. (In Slovak.)

Holko, L., Danko, M., Dóša, M., Kostka, Z., Šanda, M., Pfister, L., Iffly, J.F., 2013. Spatial and temporal variability of stable water isotopes in snow related hydrological processes. Die Bodenkultur, 64, 3–4, 39–45.

Hríbik, M., Vida, T., Škvarenina, J., Škvareninová, J. Ivan, Ľ., 2012. Hydrological effects of Norway spruce and European beech on snow cover in a mid-mountainous region of the Poľana Mts., Slovakia. J. Hydrol. Hydromech., 60, 2012, 4, 319–332. doi: 10.2478/v10098-012-0028-x.

Kattelmann, R.C., 1984. Snowmelt lysimeters: design and use. In: Proc. 52nd Annual Meeting of the Western Snow Conference, Western Snow Conference, Sun Valley, ID, pp. 68–79.

Khan, V., Holko, L., 2009. Snow cover characteristics in the Aral Sea Basin from different data sources and their relation with river runoff. Journal of Marine Systems, 76, 254–262.

Kinar, N.J., Pomeroy, J.W., 2015. SAS2: the system for acoustic sensing of snow. Hydrol. Process., 29, 4032–4050.

Kirnbauer, R., Blöschl, G., 1990. A lysimetric snow pillow station at Kühtai/Tyrol. IAHS Publ. no. 193. IAHS Press, Wallingford, pp. 173–180.

Kormos, P., Marks, D., Williams, C.J., Marshall, H.P., Aishlin, P., Chandler, D.G., McNamara, J.P., 2014. Soil, snow, subsurface storage data set from a mountain catchment in the rain–snow transition zone. Earth Systems Science Data, 6, 165–173. doi:10.5194/essd-6-165-2014.

Kostka, Z., Holko, L., 2000. Impact of climate change on runoff in a small mountain catchment. National Climatic Program of Slovak Republic, 8. Bratislava, pp. 91–109. (In Slovak.)

Kotríková, K., Hlavčová, K., Fencík, R., 2014. Changes in Snow Storage in the Upper Hron River Basin (Slovakia). Acta Silvatica et Lignaria Hungarica, 10, 2, 145–459.

Krajčí, P., Holko, L., Perdigão, R.A.P., Parajka, J., 2014. Estimation of regional snowline elevation (RSLE) from MODIS images for seasonally snow covered mountain basins. Journal of Hydrology, 519, Part B, 1769–1778.

Kuusisto, E., 1980. On the values and variability of degree-day melting factors in Finland. Nord. Hydrol., 11, 5, 235–242.

Kuusisto, E., 1984. Snow accumulation and snowmelt in Finland. Publications of the Water Research Institute, National Board of Waters, Helsinki, Finland, 55, 149 p.

Lehning, M., Völksch, I., Gustavson, D., Nguyen, T.A., Stähli, M., Zappa, M., 2006. ALPINE3D: A detailed model of mountain surface processes and its application to snow hydrology. Hydrol. Process., 20, 2111–2128.

Lehning, M., Löwe, H., Ryser, M., Raderschall, N., 2008. Inhomogeneous precipitation distribution and snow transport in steep terrain. Water Resour. Res., 44, W07404. doi: 10.1029/2007WR006545.

Liston, G.E, Sturm, M., 1998. A snow-transport model for complex terrain. Journal of Glaciology, 44, 148, 498–516.

López-Moreno, J.I., Fassnacht, S.R., Heath, J.T., Musselman, K.N., Revuelto, J., Latron, J., Morán-Tejeda, E., Jonas, T., 2013. Small scale spatial variability of snow density and depth over complex alpine terrain: Implications for estimating snow water equivalent. Adv. Water Resour., 55, 40–52.

Lundquist, J.D., Lott, F., 2008. Using inexpensive temperature sensors to monitor the duration and heterogeneity of snow-covered areas, Water Resour. Res., 44, W00D16, doi: 10.1029/2008WR007035.

Martinec, J., 1987. Meltwater percolation through an alpine snowpack In: Proc. Symp. Avalanche formation, movement and effects. IAHS Publ. No. 162. IAHS Press, Wallingford, pp. 255–264.

Merz, R., Blöschl, G., 2003. Regional flood risks – what are the driving processes? IAHS Publication No. 281, IAHS Press, Wallingford, pp. 49–58.

Mészároš, I., Miklánek, P., 2006. Calculation of potential evapotranspiration based on solar radiation income modeling in mountainous areas. Biologia, 61, Special Issue 19, S284–S288.

MIKE SHE, 2011. An integrated hydrological modelling framework, Volume 2, Reference manual, DHI, Danmark.

Mott, R., Schirmer, M., Bavay, M., Grünewald, T., Lehning, M., 2010. Understanding snow-transport processes shaping the mountain snow-cover. Cryosphere, 4, 545–559.

Nester, T., Kirnbauer, R., Parajka, J., Blöschl, G., 2012. Evaluating the snow component of a flood forecasting model. Hydrology Research, 43, 762–779.

Parajka, J., Holko, L., Kostka, Z., Blöschl, G., 2012. MODIS snow cover mapping accuracy in a small mountain catchment – comparison between open and forest sites. Hydrol. Earth Syst. Sci., 16, 2365–2377, doi: 10.5194/hess-16-2365-2012.

Pekárová, P., Halmová, D., 2009. Snow water equivalent measurement and simulation in microbasins with different vegetation cover. Journal of Hydrology and Hydromechanics, 57, 2, 88–99.

Penna, D.D., Ahmad, M., Birks, S.J., Bouchaou, L., Brenčič, M., Butt, S., Holko, L., Jeelani, G., Martínez, D.E., Melikadze, G., Shanley, J.B., Sokratov, S.A., Stadnyk, T., Sugimoto, A., Vreča, P., 2014. A new method of snowmelt sampling for water stable isotopes. Hydrol. Process., 28, 22, 5637–5644. doi: 10.1002/hyp.10273.

Pomeroy, J.W., Brun., E., 2001. Physical properties of snow In: Jones, H.G., Pomeroy, J.W., Walker, D.A., Hoham, R.W. (Eds.): Snow Ecology: an Interdisciplinary Examination of Snow-covered Ecosystems. Cambridge University Press, Cambridge, UK., pp. 45–118.

Prokop, A., 2008. Assessing the applicability of terrestrial laser scanning for spatial snow depth measurements, Cold Regions Science and Technology, 54, 3, 155–163.

Revuelto, J., López-Moreno, J.I., Azorin-Molina, C., Vicente-Serrano, S.M., 2014. Topographic control on snowpack distribution in a small catchment in the central Pyrenees: intra- and inter-annual persistence. The Cryosphere, 8, 1989–2006.

Schrödter, H., 1985. Verdunstung - Anwendungsorientierte Meßverfahren und Bestimmungsmethoden. Springer Verlag, Berlin. (In German.)

Sihvola, A., Tiuri, M., 1986. Snow fork for field determination of the density and wetness profiles of a snow pack. IEEE Transactions on Geoscience and Remote Sensing, GE24, 5, 717–721.

Tekeli, A.E., Şorman A.A., Şensoy, A., Şorman, A.Ü., 2003. Design, installation of a snowmelt lysimeter and analysis for an energy balance model studies in Turkey. In: 60th Eastern Snow Conference, Eastern Snow Conference, Sherbrooke, Quebec, Canada.

Toikka, 2013. Snow Fork – manual. Ins. toimisto Toikka Oy, Espoo, Finland, 20 p.

Vionnet, V., Brun, E., Morin, S., Boone, A., Faroux, S., Le Moigne, P., Martin, E., Willemet, J.-M., 2012. The detailed snowpack scheme Crocus and its implementation in

SURFEX v7.2. Geosci. Model Dev., 5, 773–791. doi: 10.5194/gmd-5-773-2012.

Warscher, M., Strasser, U., Kraller, G., Marke, T., Franz, H., Kunstmann, H., 2013. Performance of complex snow cover descriptions in a distributed hydrological model system: a case study for the high Alpine terrain of the Berchtesgaden Alps. Alps. Water Resour. Res., 49, 5, 2619–2637.

Weingartner, R., Barben, M., Spreafico, M., 2003. Floods in mountain areas – an overview based on examples from Switzerland. J. Hydrol., 282, 1–4, 10–24.

Wever, N., Fierz, C., Mitterer, C., Hirashima, H., Lehning, M., 2014. Solving Richards equation for snow improves snow pack meltwater runoff estimations in detailed multi-layer snowpack model. Cryosphere, 8, 1, 257–274. http://dx.doi.org/10.5194/tc-8-257-2014

Winstral, A., Elder, K., Davis, R.E., 2002. Spatial snow modeling of wind-redistributed snow using terrain-based parameters. Journal of Hydrometeorology, 3, 524–538.

Winstral, A., Marks, D., Gurney, R., 2013. Simulating wind affected snow accumulations at catchment to basin scales. Advances in Water Resources, 55, 64–79.

Zhang, F., Zhang, H., Hagen, S.C., Ye, M., Wang, D., Gui, D., Zeng, Ch., Tian, L., Liu, J., 2015. Snow cover and runoff modeling in a high mountain catchment with scarce data: effects of temperature and precipitation parameters. Hydrol. Process., 29, 52–65. doi: 10.1002/hyp.10125.

Received 5 May 2016
Accepted 8 July 2016